JACC: BASIC TO TRANSLATIONAL SCIENCE
VOL. 1, NO. 7, 2016
ISSN 2452-302X
http://dx.doi.org/10.1016/j.jacbts.2016.07.007

PRECLINICAL RESEARCH

A Transcriptomic and Epigenomic Comparison of Fetal and Adult Human Cardiac Fibroblasts Reveals Novel Key Transcription Factors in Adult Cardiac Fibroblasts

Malin K.B. Jonsson, PhD,[a] Robin J.G. Hartman, MSc,[a,b] Matthew Ackers-Johnson, PhD,[a,c] Wilson L.W. Tan, BSc,[a,c] Bing Lim, MD, PhD,[d,e] Toon A.B. van Veen, PhD,[f] Roger S. Foo, MD[a,c]

VISUAL ABSTRACT

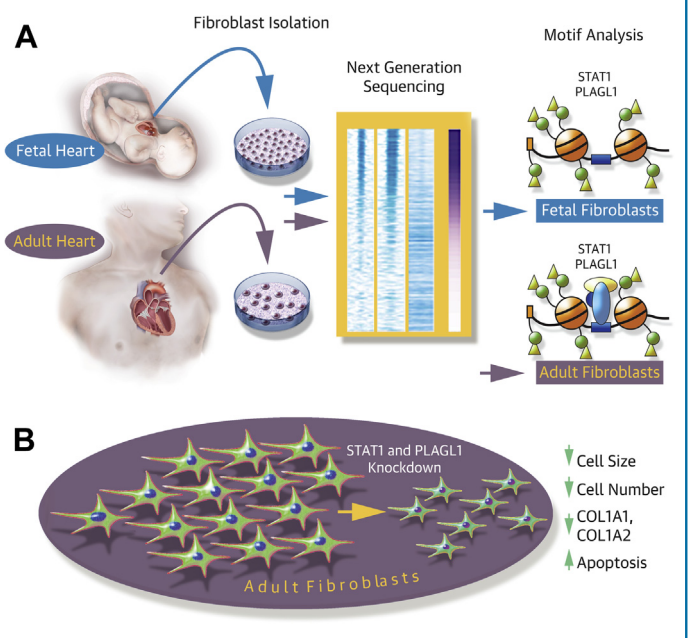

Jonsson, M.K.B. et al. J Am Coll Cardiol Basic Trans Science. 2016;1(7):590–602.

HIGHLIGHTS

- **The interplay between cardiomyocytes and cardiac fibroblasts is increasingly being recognized as important in cardiac disease.**
- **Fetal and adult cardiac fibroblasts influence their neighboring cardiomyocytes in different ways. A genome-wide comparison of the 2 reveals that they share >80% of gene transcripts.**
- **Motif analysis of empirical regulatory elements located next to differentially expressed genes led to identification of key differential regulators of fibroblast identity.**
- ***STAT1* and *PLAGL1* were identified and validated as key transcription factors to maintain the adult cardiac fibroblast phenotype. Loss of either factor led to a significant change in phenotype, including smaller cell size, apoptosis, reduced turnover, and down-regulated collagen gene expression.**

From the [a]Human Genetics, Genome Institute of Singapore, Singapore; [b]University of Utrecht, Utrecht, the Netherlands; [c]Cardiovascular Research Institute, National University Health Systems, National University of Singapore, Singapore; [d]Merck Research Laboratories, Translational Medicine Research Centre, Singapore; [e]Cancer Stem Cell Biology, Genome Institute of Singapore, Singapore; and the [f]Department of Medical Physiology, Division of Heart & Lungs, University Medical Center Utrecht, Utrecht, the Netherlands. The authors acknowledge the support from the Netherlands CardioVascular Research Initiative: the Dutch Heart Foundation, the Dutch Federation of University Medical Centres, the Netherlands Organisation for Health Research and Development, and the Royal Netherlands Academy of Sciences (CVON-PREDICT). Dr. Jonsson has received an EMBO long-term fellowship grant (EMBO ALTF 304-2012). Funding was received by Dr. Foo from the Singapore National Medical Research Council and by Drs. Foo and Lim from the Biomedical Research Council, Agency for Science, Research and Technology. All other authors have reported that they have no relationships relevant to the contents of this paper to disclose.

Manuscript received May 26, 2016; revised manuscript received July 18, 2016, accepted July 19, 2016.

SUMMARY

Cardiovascular disease remains the number one global cause of death and presents as multiple phenotypes in which the interplay between cardiomyocytes and cardiac fibroblasts (CFs) has become increasingly highlighted. Fetal and adult CFs influence neighboring cardiomyocytes in different ways. Thus far, a detailed comparison between the two is lacking. Using a genome-wide approach, we identified and validated 2 crucial players for maintaining the adult primary human CF phenotype. Knockdown of these factors induced significant phenotypical changes, including senescence and reduced collagen gene expression. These may now represent novel therapeutic targets against deleterious functions of CFs in adult cardiovascular disease. (J Am Coll Cardiol Basic Trans Science 2016;1:590–602)

ABBREVIATIONS AND ACRONYMS

aHCF = adult human cardiac fibroblast

ATAC = assay for transposase accessible chromatin

ATAC-seq = assay for transposase accessible chromatin-sequencing

CF = cardiac fibroblast

ChIP-seq = chromatin immunoprecipitation-sequencing

CM = cardiomyocyte

ECM = extracellular matrix

EMT = epithelial-to-mesenchymal transformation

FGF = fibroblast growth factor

fHCF = fetal human cardiac fibroblast

HCF = human cardiac fibroblast

IL = interleukin

IPA = Ingenuity Pathway Analysis

RNA-seq = ribonucleic acid-sequencing

RT-qPCR = reverse transcription-quantitative polymerase chain reaction

TF = transcription factor

Although cardiomyocytes (CMs) occupy most of the tissue volume and provide the mechanical force delivered by the heart, they are largely outnumbered by nonmyocyte cells (30% vs. 70%), part of which are cardiac fibroblasts (CFs) (1,2). Cross-sectional confocal microscopy of ventricular tissue reveals that each CM is in the direct vicinity of at least 1 CF (3), reflecting a significant role for CFs in the heart; that is, to create and hold a supportive environment for CMs, such as by regulation of the extracellular matrix (ECM). More than simply a "scaffold cell," CFs are understood to communicate with CMs in 3 different ways. The first method is through direct cell-to-cell contact, in which the formation of adherens junctions (cadherins) and gap junctions (connexins) play a crucial role (4). The second method is by paracrine or autocrine secretion of growth factors such as fibroblast growth factor (FGF)-2/basic FGF and transforming growth factor-β or important cytokines such as interleukin (IL)-1β and the IL-6 family, including leukemia inhibitory factor and cardiotrophin-1 (5). In the third method, cells indirectly relay signals via the ECM by modulating its composition and quantity by secretion or degradation of the ECM building blocks (4,6).

SEE PAGE 603

Common features of fibroblasts are the lack of a basement membrane, profound granular material in the cytoplasm scattered along a large Golgi apparatus, and a substantial rough endoplasmic reticulum (7). A unique marker for fibroblasts or CFs is still lacking, although both fetal and adult CF express periostin, discoidin domain receptor 2, and vimentin (8). Another feature of CFs is their ability to transform into an active state; the myofibroblast. Myofibroblasts express smooth muscle cell markers (e.g., smooth muscle actin [SMA]) and may contract. They have also been implicated in wound contraction, fibrosis, and scar healing and are a source of cytokines and growth factors, such as IL-6 and transforming growth factor-β (9).

Fibroblasts are abundant throughout all tissues in the body, and the population is heterogeneous, with diverse appearances and functions depending on where the cells reside (10). Apart from the expression of common core fibroblast genes, a specific gene expression profile involving the cardiogenic transcriptional network has been described uniquely for CFs (11). Furthermore, regional differences exist in which CFs from the atrium and the ventricle express different cardiogenic transcription factors (TFs) (11,12). Important differences have also been found between rat CFs from the embryonic heart compared with the adult heart, with a differential response in insulin-like growth factor-induced collagen production (13). The influence of CFs on co-cultured CMs also varies depending on age. Embryonic CFs increase proliferation of CMs, whereas adult CFs induce hypertrophy (6). Notably, this finding is consistent with the growth of a fetal or neonatal heart, which depends on the proliferation of CMs, whereas the adult heart responds to stress by hypertrophy. The diversity of the CF population is also underlined by the finding that CF may be derived from at least 3 sources: from the proepicardium, from endocardial- or epicardial-to-mesenchymal transformation (EMT), and from bone marrow (14–16).

Despite increasing attention to the potential role that CF may play in novel disease therapeutics (17), a detailed genome-wide characterization of the genetic and epigenetic profiles of CF has yet to be performed. In the present study, we conducted next-generation sequencing experiments with primary ventricular fetal human cardiac fibroblasts (fHCFs) and adult human cardiac fibroblasts (aHCFs) to carefully map their respective transcriptomic and epigenomic

TABLE 1 Clinical Characteristics of the fHCFs and aHCFs Used in This Study

Company	Catalog No./Lot No.	Ethnicity	Sex	Age	Clinical Profile	Site of Isolation
fHCF						
Cell Applications, Inc.	306-05f/1916	Black	Female	16 weeks gestation	Normal human fetal heart	Ventricle
Cell Applications, Inc.	306-05f/2112	Unknown	Female	21 weeks gestation	Normal human fetal heart	Ventricle
aHCF						
PromoCell	C-12375/3042901.1	White	Male	54 yrs	Histologically normal tissue	Ventricle
PromoCell	C-12375/397Z030.3	White	Female	30 yrs	Histologically normal tissue	Ventricle
PromoCell	C-12375/1051601.5	White	Male	48 yrs	Histologically normal tissue	Ventricle

Isolation methods are proprietary.
aHCFs = adult human cardiac fibroblasts; fHCFs = fetal human cardiac fibroblasts.

profiles, with the aim of unraveling key players responsible for maintaining the CF phenotype.

METHODS

Detailed Methods are available in the Supplemental Appendix. aHCFs were purchased from PromoCell (Heidelberg, Germany; catalog no. C-12375, lot no. 3042901.1, lot no. 397Z030.3 and lot no. 1051601.5), and fHCFs were purchased from Cell Applications, Inc. (San Diego, California; catalog no. 306-05g, lot no. 1916, and lot no. 2112). The fibroblasts were of ventricular origin, and all donors were free of cardiac disease. Profiling experiments were performed with human cardiac fibroblasts (HCFs) between passages 3 and 4. Cellular, molecular, and next-generation sequencing experiments were performed as described in the Supplemental Appendix. Primer

FIGURE 1 Cellular Characterization of fHCFs and aHCFs

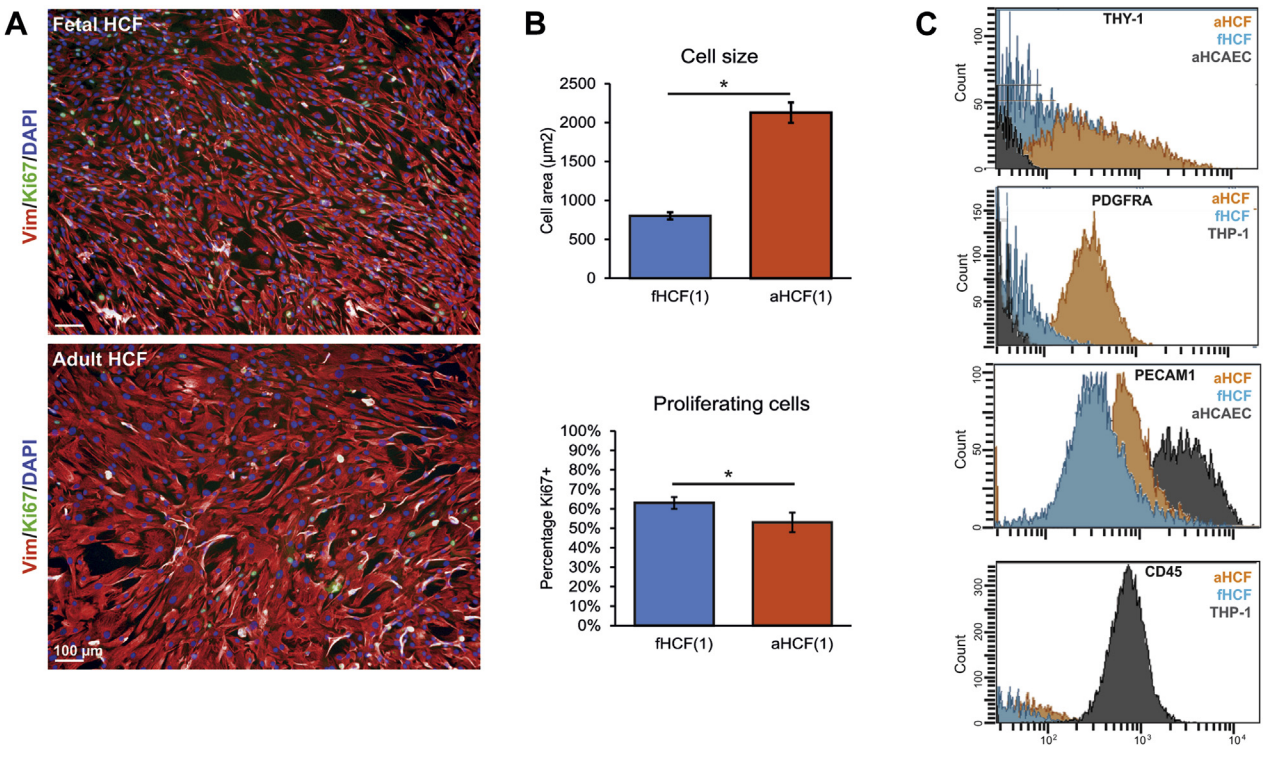

(A) Fetal human cardiac fibroblasts (fHCFs) **(top)** and adult human cardiac fibroblasts (aHCFs) **(bottom)** stained for vimentin **(red)**, Ki67 **(green)**, and 4′,6-diamidino-2-phenylindole (DAPI) **(blue)**. **(B)** Quantification to show that fHCFs are smaller in size and proliferate more than aHCFs. Values are mean ± SD; *p < 0.05, Student *t* test. **(C)** Flow cytometry analysis show that aHCFs and fHCFs express THY-1 and PDGFRA but are negative for PECAM1 and CD45. Adult human coronary artery endothelial cell (aHCAEC) or THP-1 (a human monocytic cell line) were used as control cell types.

sequences for reverse transcription-quantitative polymerase chain reaction (RT-qPCR) are listed in Supplemental Table 1.

STATISTICAL ANALYSIS. Ribonucleic acid-sequencing (RNA-seq) data were aligned to the Hg19 reference genome by using TopHat version 2.0.11 (Center for Computational Biology at Johns Hopkins University, Baltimore, Maryland). The transcriptome was assembled by using Cufflinks version 2.2.1 (Laboratory for Mathematical and Computational Biology at UC Berkeley; Computational Genomics at the Institute of Genetic Medicine at Johns Hopkins University, Baltimore, Maryland; Caltech, Pasadena), and differential expression of genes was analyzed in GENCODE gene annotation version 16 (Wellcome Trust Sanger Institute, Cambridge). Differentially expressed genes were selected on the basis of q value (false discovery rate-corrected p value) and log2fold-change produced by Cuffdiff. Chromatin immunoprecipitation-sequencing (ChIP-seq) and assay for transposase accessible chromatin-sequencing (ATAC-seq) peaks were called by using DFilter (18). Filter types for H3K4me3 and ATAC were zero mean, whereas H3K27me3 was interrogated by using a nonzero mean. Filter width settings for H3K4me3, H3K27me3, and ATAC were as follows: 8 to 10 kb, -ks = 100, -bs = 100; 1.5 to 3 kb, -ks = 25, -bs = 100; and 4 to 5 kb, -ks = 50, -bs = 100, respectively. Expected peak cutoff p values for H3K4me3, H3K27me3, and ATAC were set at 1E-6, 1E-3, and 1E-2 according to Dfilter recommendations. Peak annotation was performed by using ChIPpeakAnno (19). Known motifs and de novo motifs from ChIP-seq data were obtained by HOMER Motif Analysis (20).

Two-tailed unpaired Student *t* tests were used to assess significance in the RT-qPCR and immunostaining analysis. Results are presented as mean ± SD, and statistical significance is denoted in the graphics as $p \leq 0.05$.

RESULTS

CELLULAR CHARACTERIZATION OF CFs. fHCFs and aHCFs were characterized with the use of immunocytochemistry and flow cytometry. Clinical characteristics of the cell isolates are listed in **Table 1**. Immunocytochemical labeling was performed for vimentin and Ki67 (proliferation marker). Representative images are shown in **Figure 1A** and are quantified in **Figure 1B**. Image analysis of more than 2,000 cells in independent cultures showed that fHCFs were consistently smaller than aHCFs (802 ± 46 μm^2 vs. 2,127 ± 131 μm^2) and proliferated faster. Ki67-positive cells for fHCFs and aHCFs were 63% and 52%, respectively, representing higher proliferation in the former. A higher turnover of fHCFs compared with aHCFs was also substantiated by a shorter doubling time of 34.6 h and 68.9 h, respectively (data provided by the supplier). More than 98% of cells were α-SMA negative (Supplemental Figure 1), ensuring that the majority of the study CFs were not activated to myofibroblasts by stress conditions of cell culture. Flow cytometry results proved that both fHCFs and aHCFs expressed THY-1 and PDGFRA. Moreover, FACS also allowed us to exclude the possibility that the study cells were contaminated with other cells of endothelial (PECAM1 negative) or hematopoetic (CD45 negative) origin (**Figure 1C**).

TRANSCRIPTOMIC CHARACTERISTICS. RNA-seq was performed for both fHCFs and aHCFs (n = 3) (Supplemental Figure 2A). We used the stringent cutoff of fragments per kilobase of exon per million fragments mapped >1 to call genes expressed in both aHCFs and fHCFs. A total of 13,400 genes were expressed in both, with 1,639 and 1,354 being exclusively expressed in fHCFs and aHCFs, respectively (**Figure 2A**). Thus, aHCF and fHCF transcriptomes exhibited marked similarities, raising the important question of whether specific transcriptomic differences might define their unique phenotypic characteristics. **Figure 2B** shows a heat map of exclusively expressed genes, which expectedly segregate the 2 sets of fHCF and aHCF samples. Supplemental Appendix 2 lists all genes expressed in the 2 sets of HCFs and their corresponding expression values. Correlation comparisons between sample replicates in **Figure 2C** corroborate the distinction between aHCFs and fHCFs (correlation of fHCF replicates in blue is ~0.98, and the same for aHCF replicates in red, contrasting against lower correlations compared across fHCFs and aHCFs in purple).

We next sought to interpret gene expression signatures that distinguished between fHCFs and aHCFs and started by performing Ingenuity Pathway Analysis (IPA, Qiagen GmbH, Hilden, Germany). Supplemental Table 2 displays the highest significant genes with a log fold-change aHCF > fHCF of >4 or <-4. Using the list of differentially expressed genes, a selection was made according to manual curation for relevance on the basis of results of a thorough literature search. Selected genes were validated by using RT-qPCR (Supplemental Figure 2B) and biologically replicated in 3 additional independent HCF cell isolates (2 for adult and 1 for fetal) (Supplemental Figure 2C). Mean gene expression in aHCFs versus fHCFs by using RT-qPCR supported the RNA-seq data for all 24 genes tested.

FIGURE 2 Similarities and Differences Between the Transcriptomes of fHCFs and aHCFs

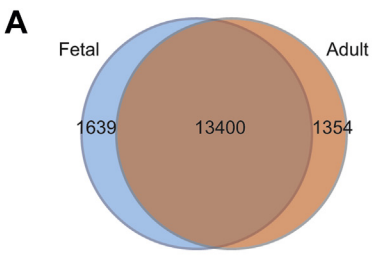

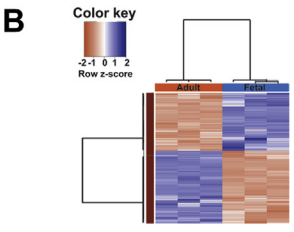

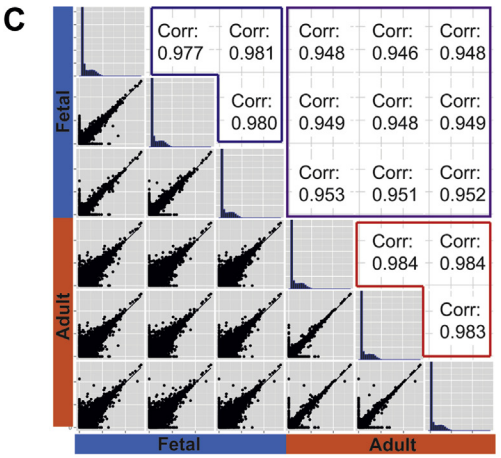

D

Adult	P-values	Fetal	P-values
Top canonical pathways			
Hepatic Fibrosis / Hepatic Stellate Cell Activation	4.96E-09	Axonal Guidance Signaling	1.39E-12
Acute Phase Response Signaling	7.24E-07	Ephrin Receptor Signaling	3.35E-09
IL-6 Signaling	2.92E-05	Hepatic Fibrosis / Hepatic Stellate Cell Activation	2.00E-07
LXR/RXR Activation	4.94E-05	IL-8 Signaling	7.30E-07
Xenobiotic Metabolism Signaling	2.18E-04	Ephrin B Signaling	3.91E-06
Physiological System Development and Function			
Immune Cell Trafficking	7.88E-06 – 3.85E-18	Cardiovascular System Development and Function	1.82E-05 – 9.32E-27
Tissue Development	1.52E-05 – 1.37E-17	Organismal Development	1.82E-05 – 7.09E-25
Cardiovascular System Development and Function	1.52E-05 – 2.06E-17	Embryonic Development	1.78E-05 – 4.34E-22
Organismal Development	1.52E-05 – 2.06E-17	Tissue Development	1.84E-05 – 4.40E-19
Skeletal and Muscular System Development and Function	1.41E-05 – 4.27E-16	Organismal Survival	6.17E-08 – 5.93E-19

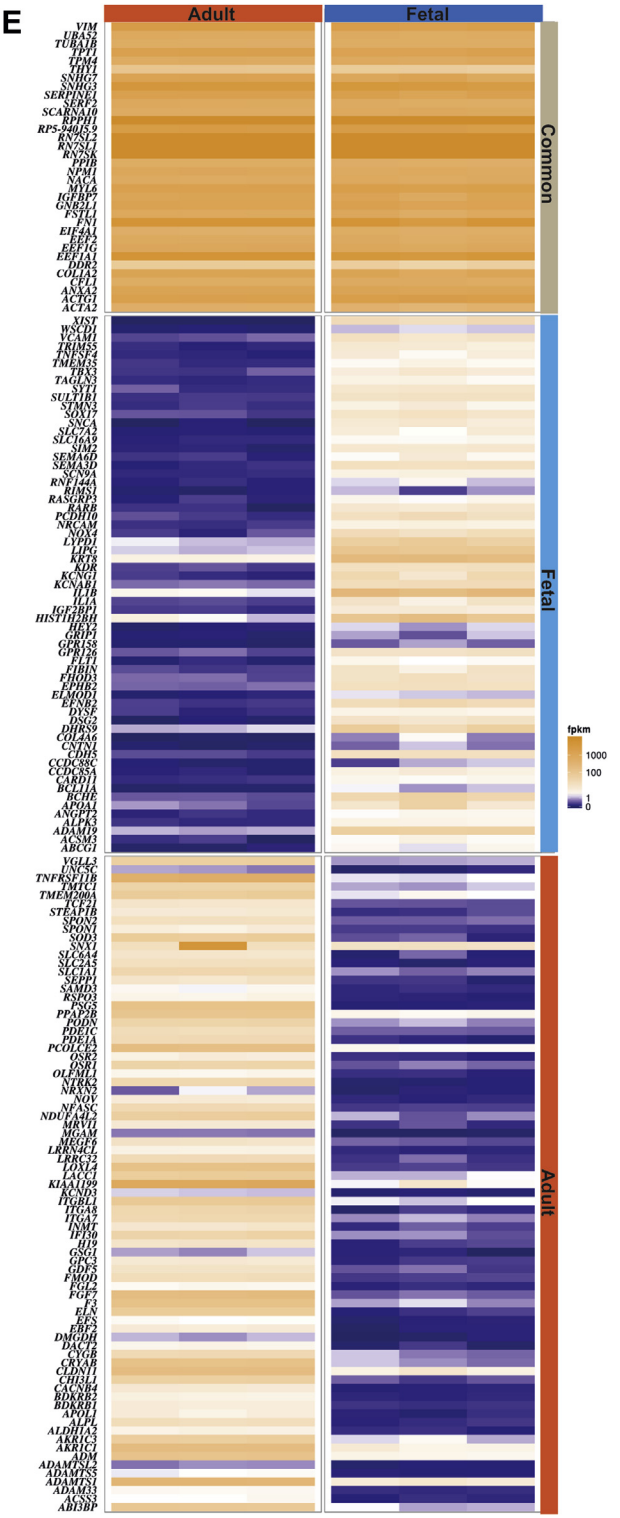

Continued on the next page

FIGURE 3 ATAC-Seq and Histone ChIP-Seq of Both Cell Types Accurately Map Out Epigenomic Profiles That Corroborate the Corresponding Transcriptomes

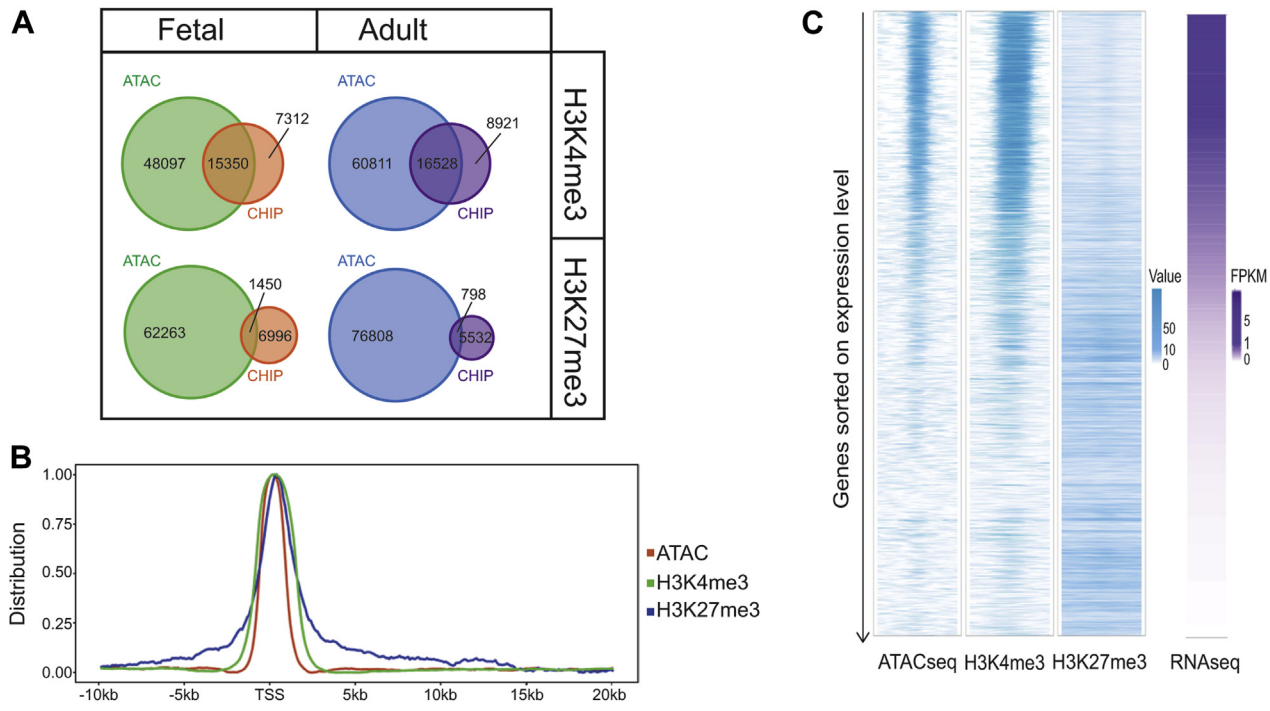

(A) Overlap of loci for assay in transposase accessible chromatin-sequencing (ATAC-seq) (open chromatin) and chromatin immunoprecipitation-sequencing (ChIP-seq) for H3K4me3 (active promoters) and H3K27me3 (repressed domains) in Venn diagrams. **(B)** Distribution of ATAC-seq and histone ChIP-seq peaks around transcription start sites (TSS) of genes. ATAC **(red)**, H3K4me3 **(green)**, and H3K27me3 **(blue)** peaks are plotted to show their enrichment around TSS. The x-axis shows the distance in kilobase centered on gene TSS; the y-axis depicts the enrichment of peaks. **(C)** Genome-wide density plots showing that ATAC-seq and H3K4me3 enrichment at TSS correspond well to genes that are highly expressed, whereas H3K27me3 are more spread out across TSS of genes that are lowly expressed. **Blue** indicates density signals for ATAC, H3K4me3, and H3K27me3 enrichment at each TSS gene locus ±5 kb represented in each row. **Purple** indicates expression level in fragments per kilobase of exon per million fragments mapped (FPKM), of the corresponding gene in each row. RNA-seq = ribonucleic acid-sequencing.

The top 1,000 differentially expressed genes on the basis of their log-fold difference were fed into IPA to perform a comparison analysis. Canonical pathway analysis of the lists revealed that genes from ephrin receptor signaling, IL-8 signaling, and Notch signaling were statistically enriched in the fetal transcriptome, whereas IL-6 signaling, among others, was enriched in the adult transcriptome. Figure 2D provides the IPA summary for the top canonical pathways and the physiological system development and functions with their respective p values. Both transcriptomes contained genes involved in tissue development and cardiovascular system development, potentially representing a common phenotype for CFs regardless of adult or fetal origins. In contrast, immune cell trafficking was an aHCF hallmark, and embryonic development was an fHCF hallmark. Gene ontology analysis for molecular functions, cellular processes, and biological processes was also consistent with the IPA pathways, and results are listed in Supplemental Figure 3. All together, we curated a list of genes to

FIGURE 2 Continued

(A) A Venn diagram of genes expressed in aHCFs **(orange)** and fHCFs **(blue)**. **(B)** Heat map of genes exclusively expressed segregating fHCFs from aHCFs. **(C)** Correlation between replicates of independent fHCF and aHCF samples (fHCF replicates in **blue box**, aHCF in **red box**, and fHCF–aHCF cross-comparison in **purple box**). **(D)** Top 5 hits of both canonical pathways analysis and physiological system development and function for transcriptomes of both aHCFs and fHCFs, with p values determined by using Ingenuity Pathway Analysis (Qiagen GmbH, Hilden, Germany). **(E)** Heat map showing representative genes that are commonly expressed in both fHCFs and aHCFs, as well as genes exclusively expressed in each. fpkm = fragments per kilobase of exon per million fragments mapped; IL = interleukin; other abbreviations as shown in Figure 1.

TABLE 2 Summary of 10 Representative Genes, Their Expression Level (RNA-Seq), and Chromatin Profiles (ATAC-Seq, H3K4me3, and H3K27me3)

	HCF	RNA-Seq	ATAC-Seq Open Chromatin	H3K4me3 Active Promoter	H3K27me3 Repressed Genomic Domain
VIM	Fetal	+++	+	+++	-
	Adult	+++	+++	+++	-
POSTN	Fetal	+++	+/-	+++	-
	Adult	++	+/-	+/-	-
HBEGF	Fetal	+	++	+++	-
	Adult	+/-	+	+	-
IL6	Fetal	++	+/-	+++	-
	Adult	+++	++	++	-
FGF7	Fetal	-	-	-	-
	Adult	++	-	++	-
ITGA8	Fetal	-	+/-	+	++
	Adult	++	++	+++	-
ELN	Fetal	-	+/-	-	+
	Adult	+	+	+++	-
CRYAB	Fetal	-	+/-	-	+
	Adult	++	+	+++	-
IL1B	Fetal	++	+	+++	-
	Adult	+/-	++	+/-	-
VCAM1	Fetal	+	+/-	+++	-
	Adult	-	+/-	+	-

The intensity of the signal is ranked from - (no signal) to +++ (strong signal) according to the criteria grouped as noted here. Ribonucleic acid-sequencing (RNA-seq): +++, >800.00; ++, 100.00 to 799.99; +, 10.00 to 99.99; +/-, 2.00 to 9.99; and -, <2.00. Assay for transposase accessible chromatin-sequencing (ATAC-seq)/histone chromatin immunoprecipitation-sequencing (ChIP-seq): +++, >15; ++, 10 to 15; +, 5 to 10; +/-, 2 to 5; and -, <2.

HCF = human cardiac fibroblast.

display those that were: 1) highly expressed in both aHCFs and fHCFs; 2) highly expressed in fHCFs but not in aHCFs; or 3) highly expressed in aHCFs but not in fHCFs (**Figure 2E**). Examples of genes differentially overexpressed in aHCFs include *FGF7, ITGA8, CRYAB, ELN*, and *TNFRSF11B,* whereas genes overexpressed in fHCFs include *IL1B, POSTN, HBEGF*, and *VCAM*.

EPIGENETIC CHARACTERISTICS: CHROMATIN ACCESSIBILITY AND HISTONE MARKS. ATAC-seq was performed to assess chromatin accessibility. Quality control of ATAC-seq libraries verified the expected nucleosomal pattern both before and after sequencing (Supplemental Figures 4A and 4B). A total of 63,829 peaks were identified for fHCFs and 77,614 for aHCFs by using criteria as detailed in the Methods section. The HCF epigenome was further characterized by mapping active and repressed gene regulatory domains using chromatin immunoprecipitation followed by next-generation sequencing (ChIP-seq) for histone marks of H3K4me3 (representing active promoters) and H3K27me3 (representing repressed genomic domains). A total of 22,662 and 25,449 peaks were detected for H3K4me3 in fHCFs and aHCFs, respectively, whereas 8,446 and 6,330 were detected for H3K27me3. By integrating the ATAC-seq loci with the 2 sets of histone ChIP-seq loci, we confirmed that ATAC-seq mainly overlaid active promoters (H3K4me3) but not repressed domains (H3K27me3) (**Figure 3A**). Analysis for the loci of ATAC, H3K4me3, and H3K27me3 revealed that all 3 signals were enriched around transcription start sites of genes (**Figure 3B**). We further integrated transcriptome (RNA-seq), ATAC-seq, and histone ChIP-seq datasets and confirmed that loci of H3K4me3 and ATAC-seq corresponded consistently with each other, representing loci of open chromatin and active promoters. In contrast, these loci differed from H3K27me3 peaks, representing repressed domains. Similarly, highly expressed genes corresponded with ATAC-seq and H3K4me3 loci but not with H3K27me3 (**Figure 3C**). As examples, the epigenomic and transcriptomic profiles of 2 genes, *ELN* (highly expressed in aHCFs) and *POSTN* (highly expressed in fHCFs), are shown in Supplemental Figures 5A and 5B. **Table 2** provides the expression profiles of some expressed genes along with their epigenetic profile.

IDENTIFICATION OF TFs FROM MOTIF ANALYSIS. Having confirmed the consistency and validity of our genome-wide transcriptomic and epigenomic profiles, we investigated whether TF regulators could be identified with an upstream role unique to aHCFs or fHCFs. A de novo motif analysis was performed with Homer on H3K4me3 loci (taken to represent active gene promoters) associated with differentially expressed genes in aHCFs and fHCFs. Two motifs and their corresponding TFs were enriched in differential H3K4me3 loci of each cell type (**Figure 4A**). Notably, the 2 TFs identified in fHCFs (*SOX17* and *SOX4*) and the 2 for aHCFs (*PLAGL1* and *STAT1*) were also strongly differentially up-regulated in their corresponding cells on the basis of their corresponding RNA-seq data. We accurately replicated these findings further in 3 (2 adult and 1 fetal) additional independent HCF cell isolates (Supplemental Figure 6A). These TFs now represent novel regulators that may play an important role in their respective cells.

TF VALIDATION BY GapmeR KNOCKDOWN. The therapeutic potential of targeting aHCFs in adult cardiac disease led us to choose *PLAGL1* and *STAT1* for validation by in vitro knockdown using GapmeR oligonucleotides. We performed this procedure in all 3 aHCF lines (**Table 1**). *PLAGL1* and *STAT1* knockdown led to >80% reduced expression levels when targeted with GapmeRs (**Figure 4B**, Supplemental Figure 6B). Interestingly, *PLAGL1* knockdown also led to reduced

FIGURE 4 TF Identification and Validation

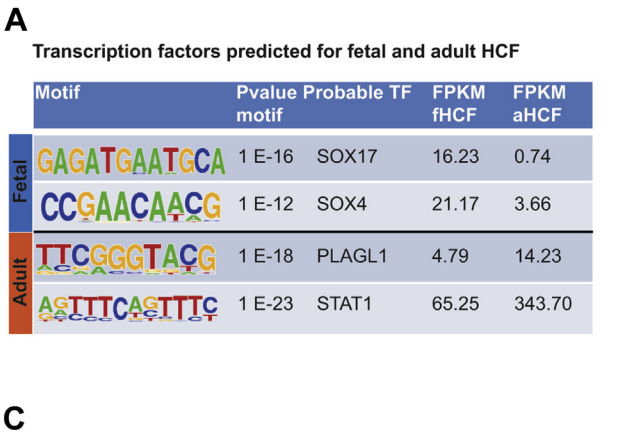

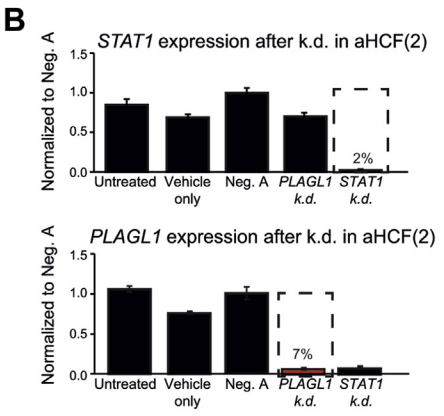

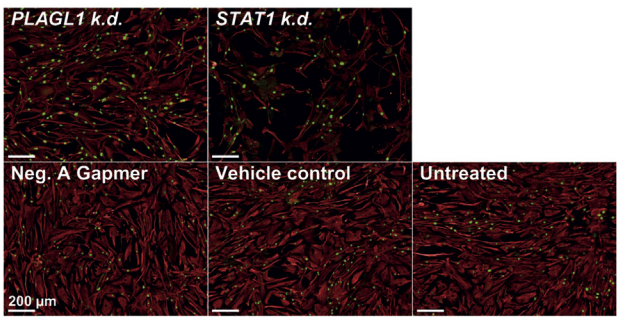

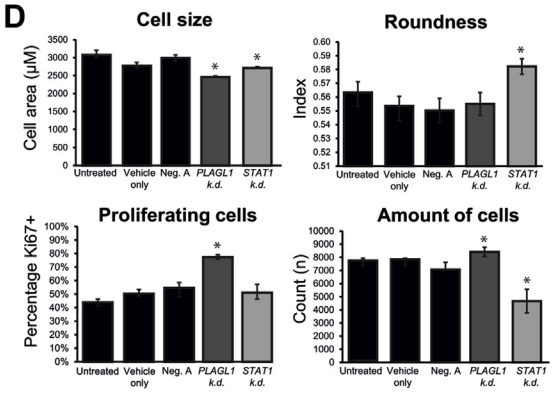

(A) Transcription factor (TF) motifs enriched at active promoters (marked by H3K4me3) of differentially expressed genes for each aHCF and fHCF. Expression of each corresponding TF gene taken from RNA-seq data is also shown. **(B)** Effective >90% GapmeR-mediated knockdown (k.d.) of *PLAGL1* and *STAT1* in aHCFs shown by reverse transcription quantitative-polymerase chain reaction, normalized to *GAPDH* and *PPIA* housekeeping gene control and subsequently to negative A (NegA) control. Values are mean ± SD. **(C)** Knockdown of either *PLAGL1* or *STAT1* leads to changes in the aHCF phenotype compared with control specimens. **(D)** Quantification of cellular parameters after knockdown of either TF shows that aHCFs become smaller and rounder after *STAT1* knockdown. *PLAGL1* knockdown also results in increased proliferation. All experiments were conducted as n = 3. Biological repeats in independent human cardiac fibroblast cell isolates are shown in Supplemental Figure 6. Values are mean ± SD. *p < 0.05 compared with NegA control. Abbreviations as shown in **Figures 1 and 3**.

STAT1 levels, suggesting an upstream effect of *PLAGL1* on *STAT1* that has not been previously reported. Negative A GapmeR construct, vehicle transfection, and nontransfected control specimens were used in all assessments. Cells were stained with antibodies against vimentin and Ki67 and analyzed for cell size, roundness, cell cycle, and cell number (n = 3). Cell size, morphology, or cell number was unchanged in all control specimens (**Figures 4C and 4D**). Instead, knockdown of *STAT1* significantly increased cell roundness, reduced cell number without increasing cell proliferation, and knockdown of either TF changed aHCF cell size (**Figure 4D**, replicated in independent cell isolates in Supplemental Figure 6C). Changes at the transcriptional level revealed that whereas *VIM* and *SMA* were unchanged, both *STAT1* and *PLAGL1* knockdown caused significant downregulation of other genes previously noted as being characteristic of the aHCF phenotype (*ELN*, *TNFRSF11B*, *COL1A1*, and *COL1A2*). Conversely, *HBEGF* associated with the fetal gene profile was upregulated (**Figure 5A**, also replicated in independent cell isolates in Supplemental Figure 6D).

To test whether knockdown fibroblasts underwent mesenchymal epithelial transition (21), key markers for epithelial cells (*CDH1*, *KRT9*, and *ATP2C2*) were quantified, but these remained poorly expressed or undetected, rejecting the possibility that this transition had taken place (Supplemental Figure 6D). We next assessed for apoptosis by using the ApopTag-Red assay. Baseline apoptosis of aHCFs in culture was 3% (untreated cells, n = 5,237), 5% (cells treated

FIGURE 5 ***STAT1*** **Knockdown Induces Fibroblast Senescence and Reduced Collagen Gene Expression**

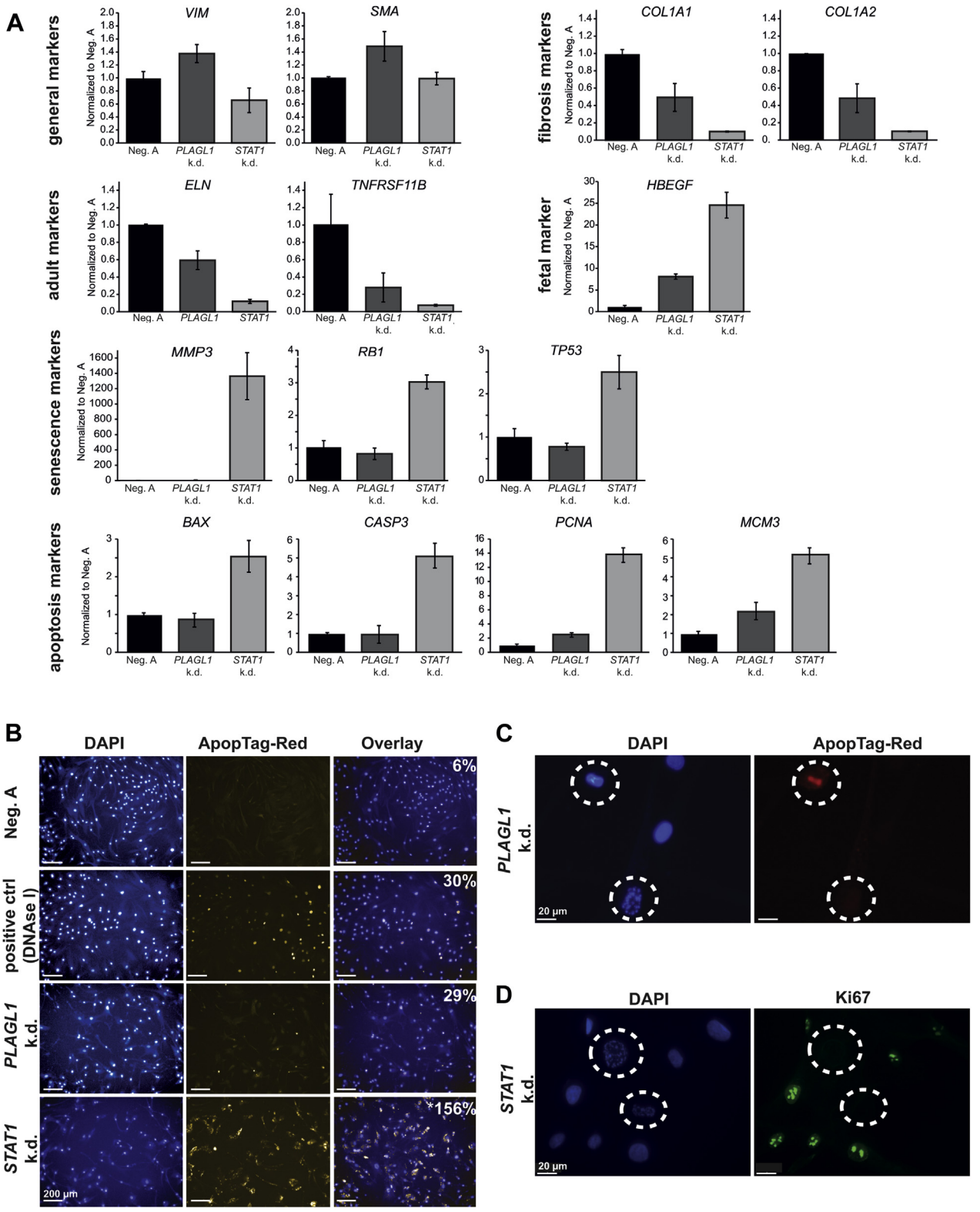

Continued on the next page

with control vehicle lipofectamine alone, n = 4,992), and 6% (cells treated with control negative A GapmeR, n = 3,710). In contrast, knockdown of *PLAGL1 or STAT1* led to significant up-regulation of apoptosis to 29% in *PLAGL1* knockdown cells (n = 2,500) and 156% in *STAT1* knockdown cells (n = 2,739; >100% apparent apoptosis is due to automated detection of multiple ApopTag-Red-stained granules in many cells) (Figure 5B).

Interestingly, apart from the classical ApopTag-Red-positive staining of nuclei to mark apoptotic cells, an overwhelming number of *STAT1* knockdown cells were also noted that showed cytoplasmic fragmentation labeling. This finding was replicated more than 3 times and was absent both in *PLAGL1* knockdown cells and in DNase1-treated positive control cells. At this time, we considered the possibility that cytoplasmic labeling represents advanced apoptosis in *STAT1* knockdown cells or evidence of widespread mitochondrial damage.

Furthermore, a significant up-regulation of the classical marker for fibroblast senescence *MMP3* (1,400-fold compared with control), as well as a subtle up-regulation of *RB1* and *TP53* (also markers of cell senescence), were noted in *STAT1* knockdown aHCFs (Figure 5A). Significant up-regulation of *MMP3* was replicated in 1 of 2 of the additional aHCF cell isolates. The third cell line instead showed a significant up-regulation of *RB1* (Supplemental Figure 6D). High-power magnification of 4′,6-diamidino-2-phenylindole-stained nuclei showed formation of heterochromatin foci in 9% of *STAT1* knockdown aHCFs (n = 5,595), whereas this outcome was not seen in untreated or positive control cells and in <1% after *PLAGL1* knockdown (n = 4,899). Cells with heterochromatin foci were frequently positive for ApopTag-Red (Figure 5C), although not all ApopTag-Red-positive cells showed heterochromatin foci. Instead, we observed a striking exclusivity in which nuclei displaying the heterochromatin foci were never positive for Ki67 (Figure 5D). Together, these findings suggest that whereas 1 subset of knockdown aHCFs undergoes apoptosis, another appears to become senescent. Furthermore, *STAT1* and *PLAGL1* knockdown led to a significant reduction in collagen *COL1A1* and *COL1A2* gene expression (Figure 5A). These results were again supported by RT-qPCR in all additional sets of aHCF cells.

DISCUSSION

Results of previous studies indicated that fHCFs and aHCFs are different in that they influence neighboring CMs in distinct ways (6,13). In the present study, we have further defined their distinct differences by performing a thorough characterization of primary fetal and adult human ventricular CFs by using cellular, molecular, and genome-wide sequencing approaches. Our results show that fHCFs are smaller and proliferate more quickly than their adult counterpart. We hypothesized that these characteristics are explained by differences in their transcriptomes and epigenomes. Indeed, genome-wide analyses of RNA-seq, ATAC-seq, and histone ChIP-seq led us to 2 TFs, highly expressed in aHCFs but not in fHCFs. We performed functional validation to conclude that they regulate aHCF cell size, cell cycle re-entry, and cell survival. Knockdown of either of the 2 TFs led to a destabilization of the aHCF phenotype and reduced gene expression of collagen genes, a major constituent of pathological fibrosis in the adult heart.

RNA-seq CONFIRMS FIBROBLAST IDENTITY AND IDENTIFIES DIFFERENTIAL SIGNALING PATHWAYS. We first confirmed that “core” genes that define a fibroblast and that are typically used as fibroblast markers, such as *VIM*, *THY1*, *DDR2*, and *COL1A2*, do not differ in expression between fHCFs and aHCFs. According to IPA analysis, 3 top functions found in the overlapping transcriptomes of the fHCFs and aHCFs are tissue development, cardiovascular system development and function, and organismal development, validating our cardiac cell source and

FIGURE 5 Continued

(A) Reverse transcription quantitative-polymerase chain reaction of representative genes after *PLAGL1* or *STAT1* knockdown in aHCFs. Whereas common human cardiac fibroblast genes *VIM* and *SMA* are unchanged, genes associated with the adult phenotype are down-regulated (*ELN* and *TNFRSF11B*), and *HBEGF* (associated with fHCFs) is up-regulated. Apoptosis-related genes such as *BAX, CASP3*, *PCNA*, and *MCM3* are in particular up-regulated after *STAT1* knockdown. Similarly, cellular senescence marker *MMP3*, as well as *RB1* and *TP53* showed strong upregulation following *STAT1* knockdown. Collagen genes (*COL1A1* and *COL1A2*) are down-regulated upon knockdown of both TFs. Values are mean ± SD and taken from at least n = 3. All $p < 0.05$, Student *t* test. Biological repeats from independent aHCF cell isolates are shown in Supplemental Figure 6. **(B)** Apoptosis was assessed by using the ApopTag-Red assay that detects DNA fragmentation. A low number of cells (6%) exhibited apoptosis under control conditions (control Neg. A GapmeR transfection), and this was significantly up-regulated in the positive control (DNAse I–treated cells) as well as after *PLAGL1* and *STAT1* knockdown. A strikingly high level of cytoplasmic ApopTag-labeling was repeatedly evident in *STAT1* knockdown cells, which was not seen in others. **(C)** Heterochromatin foci were detected in 9% (450 of 5,595 nuclei analyzed) of *STAT1* knockdown cells. These foci frequently, but not exclusively, overlapped with the ApopTag-Red stain. **(D)** Nuclei illustrating that heterochromatin foci were never found in Ki67-positive cells. Abbreviations as in Figures 1, 3, and 4.

supporting the conclusion that fHCF and aHCF transcriptomes do not differ substantially. Conversely, this finding implied that important differences would be decidedly more subtle. Nonoverlapping gene functions are embryonic development and organismal survival for fHCFs, reflecting their fetal origin (22,23), and immune cell trafficking and skeletal and muscular system development and function for aHCFs, suggesting how aHCFs may have a different role in the adult human heart compared with their fetal counterpart. We used 2 additional HCF lines to validate the RNA-seq to show that differential gene expression was confirmed across independent biological replicates. Among these are likely to be bona fide markers that can be used to distinguish between aHCFs and fHCFs.

NOVEL AND INTERESTING GENES IDENTIFIED. Differences in transcriptomes between cell types may help us to understand and explain their differential functions. For example, we expected that the fHCF transcriptome would contain genes that reveal their role for the developing heart and for inducing appropriate heart growth, whereas the aHCF transcriptome should comprise genes involved in the maintenance of a heart that is already matured. We therefore dissected the gene pathways and functions specific to each differentially expressed transcriptome for this analysis. Genes of the ephrin-receptor and ephrin b-signaling pathways were enriched in fHCFs. Indeed, ephrin B2 is important in the developing heart for ventricular chamber morphogenesis (24). Coherent to this process is the importance of Notch signaling; we also found that the Notch pathway is present in fHCFs but not aHCFs. Ephrin signaling has further been implicated for the development of vasculature (25). The finding of IL-8 signaling and ephrin signaling in fHCFs therefore suggests a role for fHCFs in vascular development as well. *VCAM-1* is among the highest differentially expressed genes in fHCFs, and *VCAM-1* has known importance for cardiac development because *Vcam1* null mice embryos do not survive past E13.5 due to retarded heart growth (23). Interestingly, *ITGA4* is also among the highest differentially expressed genes in fHCFs, and ITGA4 is an endogenous ligand for VCAM-1, creating the opportunity for inter-fHCF communication that might guide cardiac development. We also noted that analysis of gene ontology cellular processes revealed more profound plasma membrane components in fHCFs, such as integrins and other receptors, whereas aHCF-specific genes seem to focus on extracellular components. *HBEGF* is yet another gene that is highly expressed in fHCFs and lacking in aHCFs. *HBEGF* has been reported to promote cardiomyocyte proliferation in a paracrine fashion in a mouse model (6), and our data support its importance exclusively in fHCFs.

Among the top differentially expressed genes in aHCFs is *FGF7*. A gene network of FGF signaling in IPA also showed that 10 of the 15 genes involved in FGF signaling were highly differentially expressed in aHCFs, with other members of the network, including *FGF2* and *FGF14*. Although it is well established that the FGF superfamily of growth factors is important in pathophysiological processes within the cardiac environment (26), a specific role for *FGF7* has yet to be defined. Another gene more highly expressed in aHCFs was *TNFRSF11B* encoding for osteoprotegerin, a mesenchymal marker for EMT, from which a large population of adult CFs is proposed to derive (27). Overexpression of *TNFRSF11B* in rat CFs increased the expression of fibrosis-related proteins after treatment with angiotensin II, whereas its knockdown produced the reverse effect (28). *ELN* (elastin) is a third gene highly expressed in aHCFs. Elastin is a major contributor to the ECM, and it functions together with fibrillin to provide elasticity to a range of tissues (29). Interestingly, overexpression of *ELN* in cells that were transplanted to infarcted cardiac tissue in rats ameliorated the formation of scar tissue, compared with infarcted cardiac tissue that received vector-transduced cells (30). A necessity for crosslinking of elastin fibers is the presence of lysyl oxidases (29), and *LOXL4* (lysyl oxidase-like 4) is also one of the highest differentially expressed genes in aHCFs.

PUTATIVE REGULATORY TFs FOR FETAL HCFs DETERMINED BY USING MOTIF ANALYSIS. TFs determined by using de novo motif analysis add another layer of information to the regulation of the differential transcriptomes between aHCFs and fHCFs. We performed motif analysis by using active promoters, demarcated according to H3K4me3, of differentially expressed genes for either aHCFs or fHCFs, thus specifying TFs for the respective transcriptomes. Top motifs were *SOX17* and *SOX4* in fHCFs. Importantly, these TFs were also all highly expressed genes in fHCFs compared with aHCFs.

SOX17 is also expressed in endothelial cells, where it regulates angiogenesis under the influence of Notch signaling (31). Our results show that *SOX17* is expressed in fHCFs as well. *SOX4* is a master regulator of EMT and is needed for proper formation of the cardiac outflow tract (32,33). Together, the abundant expression of these 2 TFs in fHCFs suggests that they may maintain prefate determination functions, and/or that fHCFs have a role in the development of

the vasculature of the heart, similar to the ephrin and IL-8 signaling discussed earlier.

REGULATORY TFs IN aHCFs FOUND BY MOTIF ANALYSIS AND VALIDATED IN VITRO. The top 2 TFs identified for aHCFs were *PLAGL1* and *STAT1*, and their corresponding messenger ribonucleic acid was indeed significantly highly expressed in aHCFs compared with fHCFs. *PLAGL1* is an important TF in the developing heart, but its role has only been linked to CMs rather than CFs (34). In our experiments, knockdown of *PLAGL1* in aHCFs led to reduced cell size and increased apoptosis. *STAT1* activation reportedly increases fibroblast activation and collagen synthesis induced by high glucose levels (35). In our experiments, *STAT1* knockdown in aHCFs also led to reduced cell size and apoptosis. Gene expression analysis after knockdown showed that *VIM* and *SMA* levels remained unchanged, indicating that *STAT1* knockdown cells were not transforming to myofibroblasts. Instead, markers associated with the adult phenotype were down-regulated, and fetal markers were up-regulated. Together with their smaller size and increased apoptosis, we interpret these changes to represent a de-stabilization of the aHCF phenotype and viability.

We also found evidence for cell senescence based on the very high up-regulation of the classical fibroblast senescence marker *MMP3* and concomitant up-regulation of other senescence markers (*RB1* and *TP53*) (36,37). Consistent with this finding was the formation of heterochromatin foci in knockdown cells. Cells with heterochromatin foci were mutually exclusive from Ki67-positive cells, consistent with the description of senescence-associated heterochromatin foci that have already been extensively described (38). Concurrently, the expression of collagen genes *COL1A1* and *COL1A2* as well as *TNFRSF11B* were strongly down-regulated, suggesting that *STAT1* knockdown cells have a diminished ability to stimulate profibrotic processes. Importantly, these findings were confirmed in independent sets of aHCF cells from different donors.

CONCLUSIONS

Overall, this report describes for the first time important genome-wide differences between fHCFs and aHCFs. Signals from loci of active promoters led to the identification of important TFs responsible for the differential roles of HCFs. Although the exclusive use of human material limited this research to in vitro studies, these findings nevertheless reveal interesting new explanations for the different ways in which fibroblasts act in the human adult and fetal heart. Our data further suggest that this source of HCFs may be useful for translational research, such as for disease modeling of cardiac fibrosis, or for other uses, such as improving CM maturation in differentiation protocols from human embryonic stem cells. Our knockdown studies for *PLAGL1* and *STAT1* suggest their importance for aHCF viability and phenotype maintenance. Further in vivo studies will be needed to determine whether they do indeed represent potential drug targets for steering away the malevolent behavior of CFs during adult heart disease progression.

ACKNOWLEDGMENTS The authors are grateful to Zenia Tiang for assisting with library preparation for RNA-seq; to Shivaji Rikka for assistance with the Operetta high contents analysis system; and to Dr. Justus Stenzig for assistance with flow cytometry. They also highly appreciate the generosity of Professor Mark Richards and Dr. Yei-Tsung Chen, who provided the third adult HCF line aHCFs (3).

REPRINT REQUESTS AND CORRESPONDENCE: Dr. Roger S. Foo, Genome Institute of Singapore, 60 Biopolis Street, Genome #02-01, Singapore 138672, Singapore. E-mail: foosyr@gis.a-star.edu.sg.

PERSPECTIVES

COMPETENCY IN MEDICAL KNOWLEDGE: We report important genome-wide differences between fHCFs and aHCFs and identified key players responsible for maintaining the adult HCF phenotype. Our data suggest that this source of HCFs is useful in translational research, such as for disease modeling of cardiac fibrosis.

TRANSLATIONAL OUTLOOK: The transcription factors identified (*PLAGL1* and *STAT1*) may be potential drug targets for steering away the malevolent behavior of HCFs during progression of adult heart disease.

REFERENCES

1. Camelliti P, Borg TK, Kohl P. Structural and functional characterisation of cardiac fibroblasts. Cardiovasc Res 2005;65:40–51.

2. Pinto AR, Ilinykh A, Ivey MJ, et al. Revisiting cardiac cellular composition. Circ Res 2016;118:400–9.

3. Kohl P, Camelliti P, Burton FL, Smith GL. Electrical coupling of fibroblasts and myocytes: relevance for cardiac propagation. J Electrocardiol 2005;38:45–50.

4. Ottaviano FG, Yee KO. Communication signals between cardiac fibroblasts and cardiac myocytes. J Cardiovasc Pharmacol 2011;57:513–21.

5. Kakkar R, Lee RT. Intramyocardial fibroblast myocyte communication. Circ Res 2010;106:47–57.

6. Ieda M, Tsuchihashi T, Ivey KN, et al. Cardiac fibroblasts regulate myocardial proliferation through beta1 integrin signaling. Dev Cell 2009;16:233–44.

7. Snider P, Standley KN, Wang J, Azhar M, Doetschman T, Conway SJ. Origin of cardiac fibroblasts and the role of periostin. Circ Res 2009;105:934–47.

8. Lajiness JD, Conway SJ. Origin, development, and differentiation of cardiac fibroblasts. J Mol Cell Cardiol 2014;70:2–8.

9. Souders CA, Bowers SL, Baudino TA. Cardiac fibroblast: the renaissance cell. Circ Res 2009;105:1164–76.

10. Chang HY, Chi JT, Dudoit S, et al. Diversity, topographic differentiation, and positional memory in human fibroblasts. Proc Natl Acad Sci U S A 2002;99:12877–82.

11. Furtado MB, Costa MW, Pranoto EA, et al. Cardiogenic genes expressed in cardiac fibroblasts contribute to heart development and repair. Circ Res 2014;114:1422–34.

12. Burstein B, Libby E, Calderone A, Nattel S. Differential behaviors of atrial versus ventricular fibroblasts: a potential role for platelet-derived growth factor in atrial-ventricular remodeling differences. Circulation 2008;117:1630–41.

13. Diaz-Araya G, Borg TK, Lavandero S, Loftis MJ, Carver W. IGF-1 modulation of rat cardiac fibroblast behavior and gene expression is age-dependent. Cell Commun Adhes 2003;10:155–65.

14. Moore-Morris T, Guimaraes-Camboa N, Banerjee I, et al. Resident fibroblast lineages mediate pressure overload-induced cardiac fibrosis. J Clin Invest 2014;124:2921–34.

15. Ali SR, Ranjbarvaziri S, Talkhabi M, et al. Developmental heterogeneity of cardiac fibroblasts does not predict pathological proliferation and activation. Circ Res 2014;115:625–35.

16. Haudek SB, Xia Y, Huebener P, et al. Bone marrow-derived fibroblast precursors mediate ischemic cardiomyopathy in mice. Proc Natl Acad Sci U S A 2006;103:18284–9.

17. Brown RD, Ambler SK, Mitchell MD, Long CS. The cardiac fibroblast: therapeutic target in myocardial remodeling and failure. Annu Rev Pharmacol Toxicol 2005;45:657–87.

18. Kumar V, Muratani M, Rayan NA, et al. Uniform, optimal signal processing of mapped deep-sequencing data. Nature Biotechnol 2013;31:615–22.

19. Zhu LJ, Gazin C, Lawson ND, et al. ChIPpeakAnno: a bioconductor package to annotate ChIP-seq and ChIP-chip data. BMC Bioinformatics 2010;11:237.

20. Heinz S, Benner C, Spann N, et al. Simple combinations of lineage-determining transcription factors prime cis-regulatory elements required for macrophage and B cell identities. Mol Cell 2010;38:576–89.

21. Li R, Liang J, Ni S, et al. A mesenchymal-to-epithelial transition initiates and is required for the nuclear reprogramming of mouse fibroblasts. Cell Stem Cell 2010;7:51–63.

22. Acharya A, Baek ST, Huang G, et al. The bHLH transcription factor Tcf21 is required for lineage-specific EMT of cardiac fibroblast progenitors. Development 2012;139:2139–49.

23. Kwee L, Baldwin HS, Shen HM, et al. Defective development of the embryonic and extraembryonic circulatory systems in vascular cell adhesion molecule (VCAM-1) deficient mice. Development 1995;121:489–503.

24. Grego-Bessa J, Luna-Zurita L, del Monte G, et al. Notch signaling is essential for ventricular chamber development. Dev Cell 2007;12:415–29.

25. Zhang J, Hughes S. Role of the ephrin and Eph receptor tyrosine kinase families in angiogenesis and development of the cardiovascular system. J Pathol 2006;208:453–61.

26. Itoh N, Ohta H. Pathophysiological roles of FGF signaling in the heart. Front Physiol 2013;4:247.

27. Smith CL, Baek ST, Sung CY, Tallquist MD. Epicardial-derived cell epithelial-to-mesenchymal transition and fate specification require PDGF receptor signaling. Circ Res 2011;108:e15–26.

28. Shen A, Hou X, Yang D, et al. Role of osteoprotegerin and its gene polymorphisms in the occurrence of left ventricular hypertrophy in essential hypertensive patients. Medicine (Baltimore) 2014;93:e154.

29. Kielty CM, Sherratt MJ, Shuttleworth CA. Elastic fibres. J Cell Sci 2002;115:2817–28.

30. Mizuno T, Mickle DA, Kiani CG, Li RK. Overexpression of elastin fragments in infarcted myocardium attenuates scar expansion and heart dysfunction. Am J Physiol Heart Circ Physiol 2005;288:H2819–27.

31. Lee SH, Lee S, Yang H, et al. Notch pathway targets proangiogenic regulator Sox17 to restrict angiogenesis. Circ Res 2014;115:215–26.

32. Tiwari N, Tiwari VK, Waldmeier L, et al. Sox4 is a master regulator of epithelial-mesenchymal transition by controlling Ezh2 expression and epigenetic reprogramming. Cancer Cell 2013;23:768–83.

33. Schilham MW, Oosterwegel MA, Moerer P, et al. Defects in cardiac outflow tract formation and pro-B-lymphocyte expansion in mice lacking Sox-4. Nature 1996;380:711–4.

34. Yuasa S, Onizuka T, Shimoji K, et al. Zac1 is an essential transcription factor for cardiac morphogenesis. Circ Res 2010;106:1083–91.

35. Dai B, Cui M, Zhu M, Su WL, Qiu MC, Zhang H. STAT1/3 and ERK1/2 synergistically regulate cardiac fibrosis induced by high glucose. Cell Physiol Biochem 2013;32:960–71.

36. Rodier F, Campisi J. Four faces of cellular senescence. J Cell Biol 2011;192:547–56.

37. Young AR, Narita M. SASP reflects senescence. EMBO Rep 2009;10:228–30.

38. Narita M, Nunez S, Heard E, et al. Rb-mediated heterochromatin formation and silencing of E2F target genes during cellular senescence. Cell 2003;113:703–16.

KEY WORDS cardiac fibroblasts, collagen, histone methylation, transcriptome

APPENDIX For supplemental material including tables and figures, please see the online version of this article.